NJC

ROYAL SOCIETY OF CHEMISTRY

PAPER

View Article Online
View Journal | View Issue

Cite this: *New J. Chem.*, 2025, **49**, 20462

Nucleophilic reactivity of terminal amino groups of PAMAM dendrimers

Alejandra P. López-Pacheco, Elizabeth Alpizar-Juárez, Paola Gómez-Tagle * and Anatoly K. Yatsimirsky *

Received 27th June 2025,
Accepted 7th November 2025

DOI: 10.1039/d5nj02642c

rsc.li/njc

Kinetics of aminolysis of 4-nitrophenyl acetate and 2,4-dinitrofluorobenzene by PAMAM dendrimers of four generations (G0, G1, G3 and G4) and a reference compound, *N*-acetyl ethylenediamine (AcEn), have been studied within a pH range of 6 to 11. Observed rate constants per one amino group for dendrimers are close to those for AcEn at high pH but in neutral solutions a 10-fold dendritic effect is observed with both substrates. For G0 and G1 the individual rate constants of dendrimer species in different protonation states were determined analyzing the pH-rate profiles by multiple linear regression using the species distribution diagrams obtained from the potentiometric titrations of dendrimers. Although the protonation of dendrimers induces a decrease in pK_a values of protonated amino groups, the rate constants remain unaffected by protonation and the dendritic effect can be attributed entirely to an increased relative fraction of neutral amino groups in partially protonated species due to a decrease in pK_a. A similar conclusion can be drawn for G3 and G4 dendrimers analyzing the dependencies of the observed rate constants based on potentiometrically determined concentrations of free amino groups at variable pH. The reaction with 2,4-dinitrofluorobenzene can be used for a quantification of dendrimers in a μM concentration range in DMSO solution.

Introduction

Dendritic catalysis rapidly developed into a prominent area soon after discovery of dendrimers.[1] Currently it is considered as a type of biomimetic[2] or supramolecular catalysis.[3] Among others, biologically important ester cleavage reactions promoted by dendritic nucleophiles or organic catalysts incorporated into a dendritic structure have been studied as enzyme mimics or as the test reactions to establish some general principles of dendritic catalysis.[4] Typically, dendrimers are used as carriers of covalently attached reactive entities however the intrinsic nucleophilic reactivity of terminal amino groups of unmodified PAMAM dendrimers has also attracted attention.[1,3a,5]

In the first example of such a system, a small PAMAM-type dendrimer was used in the kinetic study of the aminolysis of substituted phenyl acetates.[6] The reactivity of the dendrimer per amino function toward the cleavage of 4-nitophenyl acetate (NPA) was similar to that measured for different simple polyamines like ethylenediamine, diethylenetriamine, *etc.* In more recent studies, the rate of NPA cleavage was measured with a series of commercial PAMAM dendrimers of generations from G0 to G4 (4 to 64 terminal amino groups) in comparison with a reference compound, *N*-acetyl ethylenediamine (AcEn), chosen as a control because of its chemical similarity to the external domain of dendrimers.[7] A large 28-fold rate enhancement attributed to the hydrophobic binding of the substrate and transition state stabilization effects was claimed with the third-generation dendrimer G3. This important study confirms that NPA undergoes the aminolysis rather than in principle possible hydrolysis in the presence of dendrimers, however, conclusions regarding the dendritic effect rely on a limited set of experimental results: all measurements are performed at a single pH 8.5 and at a single concentration of dendrimers and no attempt is made to assign the esterolytic reactivity of amino groups to the individual ionization states of the dendrimers.

More detailed kinetic studies of ester aminolysis performed with non dendrimeric polyamines poly(ethyleneimine)[8] and polyallylamine[9] were focused on the analysis of pH-profiles of the reaction rates in terms of Brønsted correlations: rate constants with apparent pK_a values (pK_{app}) of protonated amino groups calculated at variable pH in accordance with eqn (1), where α is the fraction of free amino groups calculated from the results of potentiometric titrations of polymers.

$$pK_{app} = pH + \log\{(1 - \alpha)/\alpha\} \quad (1)$$

Protonation of polyamines caused a decrease in pK_{app} due to a set of short-ranged and long-ranged interactions between protonated and neutral amino groups. Interestingly, the

Facultad de Química, Universidad Nacional Autónoma de México, 04510, Mexico. E-mail: pao@unam.mx, iatsimirski46@comunidad.unam.mx

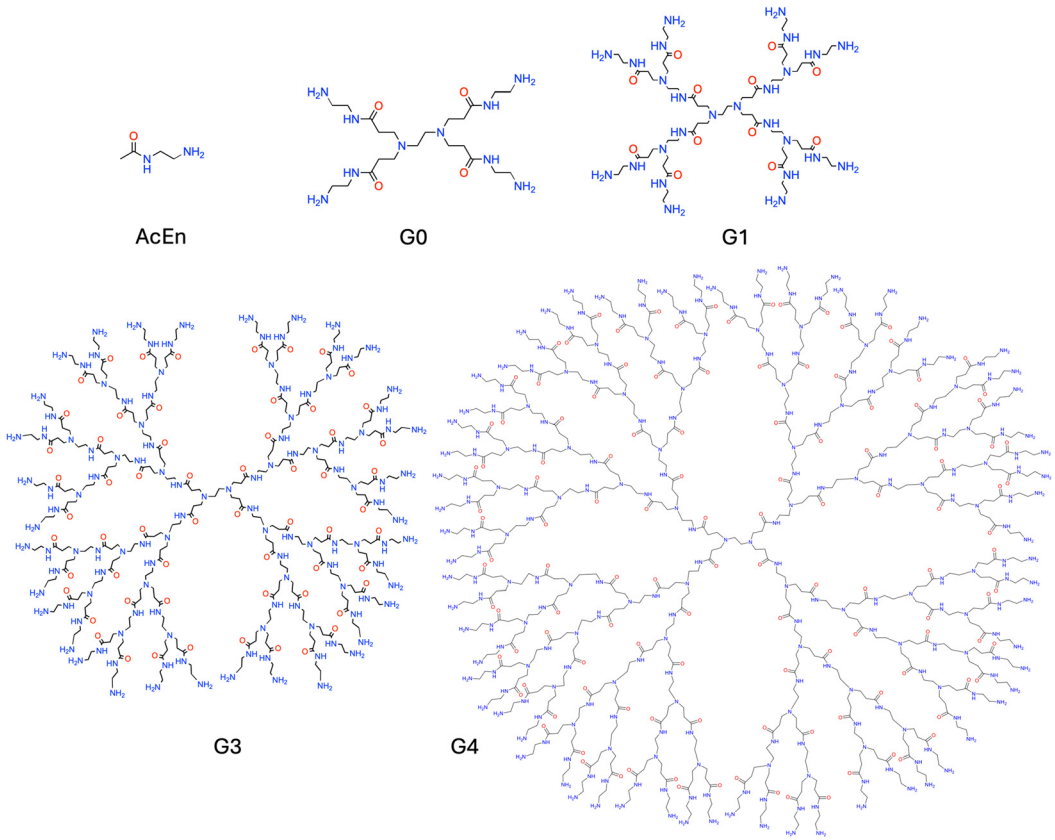

Chart 1 Chemical structures of the poly(amidoamine) (PAMAM) dendrimers for generations G0, G1, G3 and G4 employed in this study.

Brønsted plots constructed with pK_{app} demonstrated similar slopes as those obtained with low molecular weight amines of variable basicities. It would be interesting to see whether such behavior is observed also with dendrimers.

In contrast to common polyamines with variable distances between amino groups and disordered conformation of polymer chains, PAMAM dendrimers possess regular structures (see Chart 1). Ionization equilibria and distribution of neutral and protonated amino groups in these dendrimers were studied in large details[10–13] creating the basis of a meaningful interpretation of kinetic results. The major purpose of this study is to analyze the trends in nucleophilic reactivity of PAMAM terminal amino groups as a function of the degree of protonation of dendrimers affecting not only the accessibility -and possibly the basicity- of reactive nucleophilic groups, but also the size and three-dimensional structure of dendrimers,[14] which in turn should influence their properties such as reactivity, intermolecular interactions and based on these, their catalytic and drug delivery properties.

Two nucleophilic substitution reactions were studied in this work: NPA aminolysis, which is a type of nucleophilic acyl substitution reaction, and the aminolysis of 2,4-dinitrofluorobenzene (DNFB), which is a type of aromatic nucleophilic substitution (S_NAr) reaction. Both reactions have several common aspects (Scheme 1): at the first step they involve addition of amine nucleophile to sp^2 carbon changing its hybridization to sp^3 with the formation of the respective tetrahedral zwitterionic intermediate followed by the elimination of the leaving group and the restoration of sp^2 carbon hybridization. The essential difference is that, in the case of an S_NAr reaction, the negative charge of the zwitterion is strongly delocalized, accompanied by a loss of aromaticity of the substrate. An additional possible step, omitted in Scheme 1, is the deprotonation of the tetrahedral intermediate, which is manifested by a contribution of general base catalysis often provided by an excess of the amine itself. In water this reaction path is low efficient for acyl substitution and not observed for S_NAr reactions, although it is essential in aprotic solvents.[15–17] Both reactions proceed with primary and secondary amines, but no with tertiary amines which can only participate as general base catalysts facilitating the proton transfer from the tetrahedral intermediate.

The reaction of DNFB, also known as Sanger reagent, with amines is an important analytical procedure widely used in protein analysis, spectrophotometric determination of amino acids, primary and secondary amines in biological samples and drugs; aminoglycoside antibiotics; and as the derivatization reagent in HPLC.[18] The method has significant drawbacks such as a long reaction time, the necessity of heating and the removal of the hydrolysis by-product, 2,4-dinitrophenol. During this study a significant improvement of the analytical procedure was achieved and a simple and fast spectrophotometric method of determination of PAMAM dendrimers in a μM range was proposed. The chemical structures of dendrimers and the reference compound used in this study are shown in Chart 1.

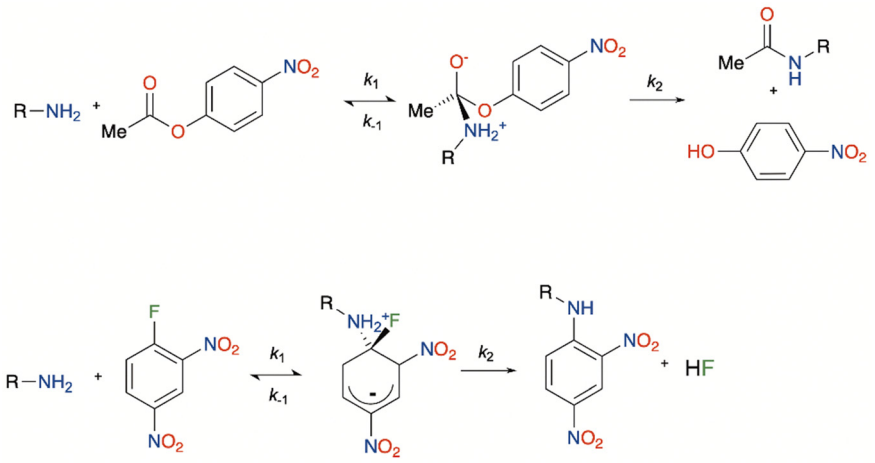

Scheme 1 Mechanisms of aminolysis of NPA and DNFB.

Results and discussion

1. Acid–base properties and speciation of dendrimers used in this study

At the first step of this study, PAMAM-NH_2 dendrimers G0, G1, G3 and G4 were characterized by potentiometric acid–base titrations performed in both directions of the pH scale for verifying they were reversible and using about 10 mM of total amine concentration where interactions dendrimer–dendrimer are negligible.[10] Representative titration plots are shown in Fig. 1–3 and a complete set of potentiometric data together with fitting results are given in (Tables S3–S9 and Fig. S2–S7). Stepwise deprotonation constants for dendrimers G0 and G1 were determined by fitting simultaneously several titration curves for a given dendrimer with Hyperquad. Table 1 collects all pK_a values for this two dendrimers which are in good agreement with previously reported values.[10–13] Interestingly, there is also a good agreement with the predicted values for dendrimers G0 and G1 with ACD pK_a software using both available algorithms, Classic and Galas (Table S9). Based on known pK_a values, one can calculate the distribution of differently protonated species at variable pH, also illustrated in Fig. 1 and 2, and attribute the observed reactivity to individual protonated forms of a dendrimer. For dendrimers G3 and G4 the number of pK_a values increases to the point where it is no longer possible to fit the titration curves nor calculate the species distribution, so the analysis of our kinetic results for these dendrimers was performed in a simpler way guided by a more in-depth quantitative analysis of the results for G0 and G1.

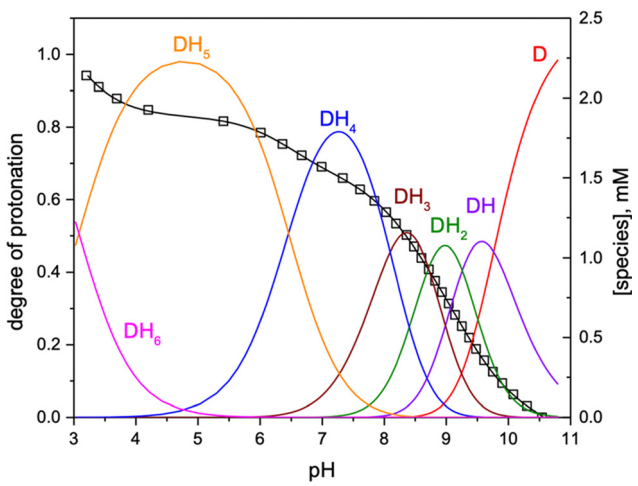

Fig. 1 Degree of protonation of amino groups from potentiometric titration (open squares left *Y*-axis) of 2.4 mM G0 by HCl, superimposed with the species distribution plots (right *Y*-axis). From left to right the fully protonated dendrimer DH_6 (magenta line) to the neutral dendrimer D (red line). The black solid line is the theoretical fit calculated by Hyperquad.

According to a comprehensive general model of protonation equilibria of poly(amidoamine) dendrimers developed by Borkovec *et al.*[10] the initial protonation of dendrimers involves the external primary amino groups and only after the complete protonation of the external groups do the internal tertiary amino groups become protonated as well. For dendrimers of larger generation such behavior is manifested in a clearly observed plateau about 50% of protonation, as can be seen in Fig. 3(a) and (b) for G3 and G4. In the case of the smaller dendrimers G0 and G1 one can observe less pronounced but still noticeable plateau regions at 65% and 60% of protonation, respectively (Fig. 1 and 2) corresponding to their fractions of primary amino groups. These plateau regions are observed at pH about 7 for all dendrimers. With G0 and G1 it is evident that these regions also coincide with maximum abundances of species with fully protonated primary amino groups: DH_4 for G0 and DH_8 for G1 (blue line in Fig. 1 and 2) observed at pH 7.2 and 7.4 respectively. Thus, the protonation of reactive primary amino groups and unreactive tertiary amino groups occurs in different pH regions which makes it easy to estimate the concentration of primary amino groups from potentiometric titration data.

2. Nucleophilic reactivity of *N*-acetyl ethylenediamine

N-Acetyl ethylenediamine (AcEn) was used in this work as the reference compound to analyze possible dendritic effects in the

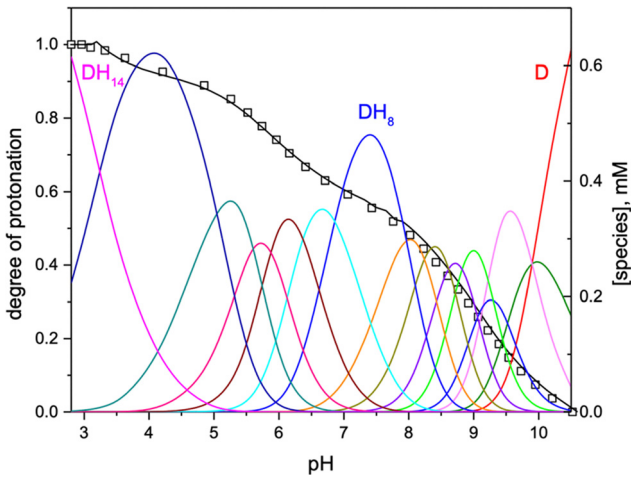

Fig. 2 Degree of protonation of amino groups from potentiometric titration (open squares left *Y*-axis) of 0.87 mM G1 by HCl, superimposed with the species distribution plots (right *Y*-axis). From left to right the fully protonated dendrimer DH_{14} (magenta line) to the neutral dendrimer D (red line). The black solid line is the theoretical fit calculated by Hyperquad.

reactivity of PAMAM dendrimers of various generations. The $pK_a = 9.37 \pm 0.01$ for protonated AcEn was determined by potentiometric titrations (Tables S1, S2 and Fig. S1). The observed second-order rate constants for NPA cleavage, k_2', by AcEn were determined at variable pH (Fig. 4(a)) from the slopes of observed first-order rate constants $k_{1,obs}$ *vs.* total AcEn concentration (Fig. S14) and the second-order rate constant $k_{2,Nu} = 0.88 \pm 0.03\ M^{-1}\ s^{-1}$ corresponding to the reaction with completely deprotonated amino group of AcEn, was calculated from these results through fitting to the theoretical eqn (2). The value of the "kinetic" $pK_a = 9.37 \pm 0.07$ calculated from the fitting of the profile in Fig. 4(a), coincided with the pK_a value determined potentiometrically.

$$k_2' = k_{2,Nu}/(1 + [H^+]/K_a) \quad (2)$$

Rate constants for the aminolysis of NPA follow a linear Brønsted dependence.[19] Table S10 contains reported $k_{2,Nu}$ values for a series of primary amines and Fig. 5(a) illustrates the respective Brønsted plot with the slope $\beta_{Nuc} = 0.83 \pm 0.04$. The point for AcEn shown as a red square perfectly lays on the plot with other primary amines confirming the correctness of the determined $k_{2,Nu}$ value.

Table 1 Stepwise deprotonation constants of dendrimers G0 2.5 mM and G1 1.25 mM determined by potentiometric titrations

	pK_a, G0				pK_a, G1	
Species	This work	Ref. 10	Ref. 11	Ref. 13	This work	Ref. 10
DH	9.76 ± 0.02	9.70	9.69	9.78	9.92 ± 0.24	9.95
DH_2	9.26 ± 0.02	9.26	9.15	9.24	9.89 ± 0.21	9.70
DH_3	8.65 ± 0.02	8.74	8.69	8.84	9.16 ± 0.63	9.25
DH_4	8.09 ± 0.03	8.31	8.21	8.35	9.29 ± 0.46	9.19
DH_5	6.46 ± 0.05	6.68	6.57	6.64	8.83 ± 0.16	8.78
DH_6	3.08 ± 0.09	3.15	3.19	2.77	8.61 ± 0.40	8.68
DH_7					8.24 ± 0.15	8.30
DH_8					7.95 ± 0.23	7.96
DH_9					6.87 ± 0.08	7.10
DH_{10}					6.67 ± 0.16	6.36
DH_{11}					5.88 ± 0.20	5.95
DH_{12}					6.00 ± 0.12	5.55
DH_{13}					5.02 ± 0.05	5.10
DH_{14}					3.24 ± 0.10	3.07

The corresponding pH-profile for the reaction of AcEn with DNFB is given in Fig. 4(b). The fitting to the eqn (2) affords $k_{2,Nu} = 0.31\ M^{-1}\ s^{-1}$ with a "kinetic" $pK_a = 9.22 \pm 0.04$ close to the potentiometrically determined value. Comparison of these results with reported data for DNFB aminolysis[16,17,20] was again performed in terms of a Brønsted correlation. Table S11 collects the reported rate constants for primary amines and Fig. 5(b) shows the Brønsted plot, with the point for AcEn shown as a red square, and the slope $\beta_{Nuc} = 0.49 \pm 0.05$.

3. NPA aminolysis by dendrimers

The reactivity of dendrimer amino groups was expressed in terms of the second-order rate constants $k_2' = k_{1,obs}/[\text{total primary amino groups}]$. The values of k_2' at variable pH for all dendrimers and AcEn are shown in Fig. 6(a). The profiles of k_2' *vs.* pH have a characteristic shape, increasing in accordance with increase in the fraction of free amino groups and "saturating" at high pH, above the pK_a, when the fraction of amino groups approaches unity and k_2'

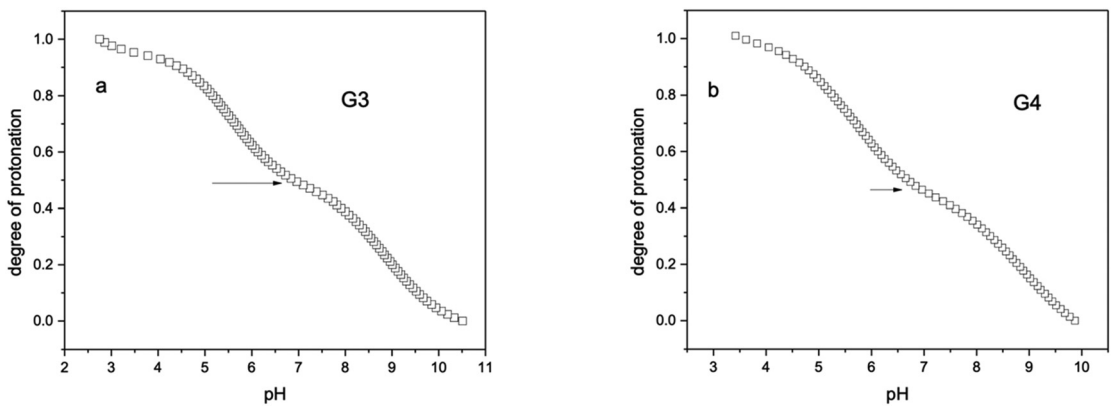

Fig. 3 Potentiometric titrations of (a) 0.62 mM G3 and (b) 0.13 mM G4 by HCl. Arrows indicate the positions of plateau regions.

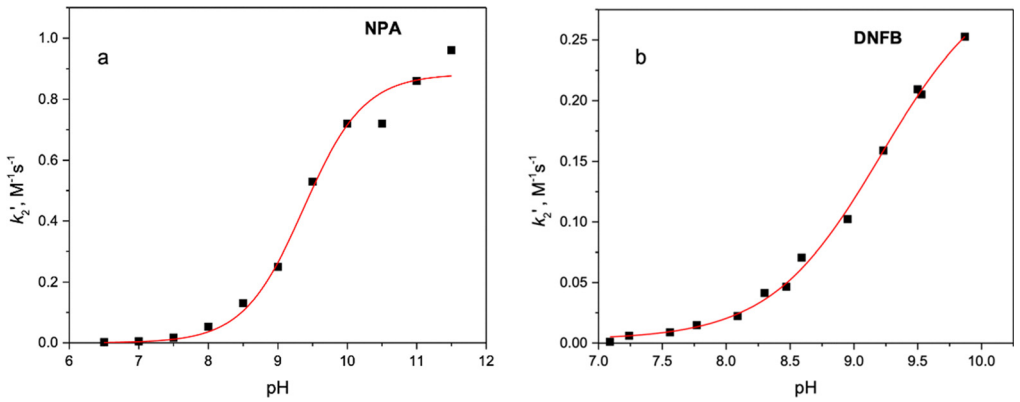

Fig. 4 pH-rate profiles for reactions of AcEn with (a) NPA and (b) DNFB.

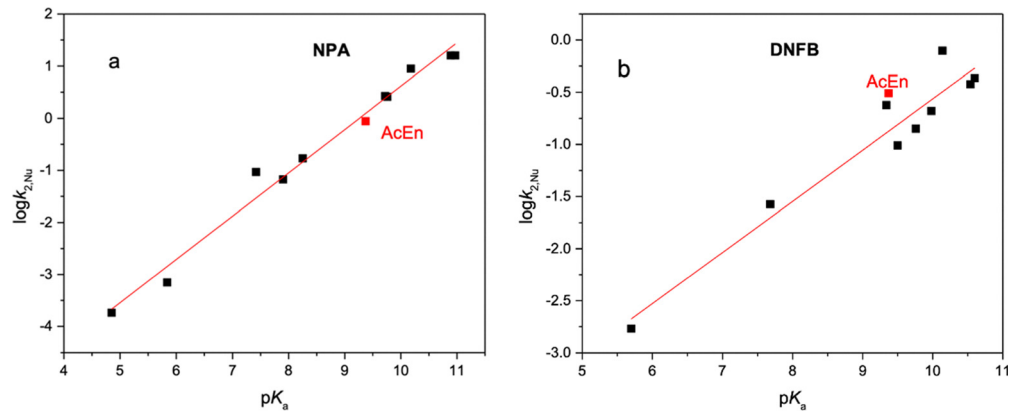

Fig. 5 The Brønsted plots for reactions of primary amines with (a) NPA and (b) DNFB.

becomes equal to $k_{2,Nu}$. Although, the $k_{2,Nu}$ values for their fully neutral forms are very close for all dendrimers and AcEn, a "dendritic effect" exists, at lower pH, when dendrimers became partially protonated, reaching a maximum value of *ca.* 15-fold for G3 and G4 around pH 7. The partial protonation of the dendrimers induces a decrease in the pK_a of protonated amino groups (see Table 1) with a consequent increase in their degree of ionization at a given pH. Therefore, at a given pH value within the pH range below the first pK_a (about 10) one observes an increase in the fraction of reactive free amino groups as compared to AcEn possessing a higher and constant pK_a value. This is illustrated in Fig. 6(b), which demonstrates a clear correlation of this effect and the pH-rate profiles implying that the free amino groups retain their intrinsic reactivity in the

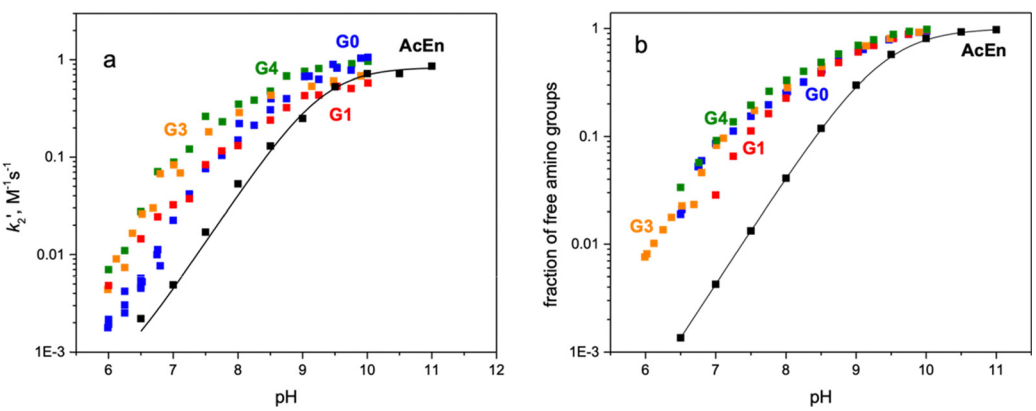

Fig. 6 (a) Observed second-order rate constants per total amino groups, k_2' M^{-1} s^{-1}, of NPA aminolysis by dendrimers and AcEn *vs.* pH; (b) fraction of free amino groups *vs.* pH.

partially protonated dendrimer species as it will be proved below.

A quantitative analysis of pH-profiles for G0 and G1 was performed using the corresponding species distribution diagrams. Fig. 7 shows the distribution of DH_n species (n = 0–4) (left vertical axis) over the pH range 6–10, where the rate of NPA aminolysis is experimentally measurable. This distribution pattern is superimposed with the pH profile of the observed first-order rate constants ($k_{1,obs}$, right vertical axis). For the quantitative analysis leading to the attribution of the meaningful nucleophilic rate constants $k_{2,Nu}$ to individual protonated dendrimer species, $k_{1,obs}$ was expressed as the sum of contributions from the differently protonated species DH_n (n = 0–3) each providing 4–n free amino groups reacting with their corresponding second-order rate constants $k^n_{2,Nu}$.

$$k_{1,obs} = \sum_{n=0}^{3} k^n_{2,Nu}(4-n)[DH_n] \quad (3)$$

The concentrations of DH_n species were calculated with HYSS program for each pH, using the pK_a values listed in Table 1. The rate constants $k^n_{2,Nu}$ were calculated by multiple linear regression using eqn (3). The resulting $k^n_{2,Nu}$ values, associated with the pK_a values of respective protonated dendrimer species are collected in Table 2. The black solid line in Fig. 7 is the theoretical calculated profile of $k_{1,obs}$ *vs.* pH with eqn (3) and rate constants given in Table 2.

Although the $k^n_{2,Nu}$ values for increasing n refer to progressively less basic amino groups and according to the Brønsted plot (Fig. 5(a)) the decrease in pK_a from 9.16 to 8.09 should produce approximately a 10-fold decrease in $k^n_{2,Nu}$, the experimental values are essentially constant equaling on average 1.16 ± 0.05 M^{-1} s^{-1}. This represents a small 30% increase in the reactivity of dendrimer amino groups compared to the reference compound AcEn, which may be attributed to a medium effect or a weak attraction of the hydrophobic NPA molecule to dendrimers.

A similar analysis for G1 dendrimer was performed in terms of eqn (4). The species distribution diagram, along with the superimposed rate constant – pH profile, is shown in Fig. 8. In this case, the number of fitting parameters was too large for a meaningful multiparametric regression analysis. For this reason, the approximate values of $k^n_{2,Nu}$ were estimated by a manual iteration process. In the first step, the theoretical profile was calculated assuming that, like in the case of G0, all species possess similar $k^n_{2,Nu}$ values of 0.67 M^{-1} s^{-1} estimated from results obtained at high pH. This profile is shown as a dashed line in Fig. 8 and it clearly underestimates the $k_{1,obs}$ values for the protonated species. Subsequently, the profiles were calculated with $k^n_{2,Nu}$ values gradually increased for higher n. The optimal fit, shown as a black solid line in Fig. 8, was obtained with a set of $k^n_{2,Nu}$ values listed in Table 2, which are slightly increased by *ca.* 10% for tri- to hexa- protonated species, and strongly increased for a hepta- protonated species. The reason for this effect is not clear. A possible explanation involves general acid assistance by ammonium groups, which could stabilize the alkoxide oxygen of the zwitterionic intermediate or facilitate the departure of the leaving group but is unlikely for an ester with such a good leaving group as 4-nitrophenol. A more plausible explanation arises from considering a conformational effect of protonation making *e.g.* more accessible the reactive amino groups.

$$k_{1,obs} = \sum_{n=0}^{7} k^n_{2,Nu}(8-n)[DH_n] \quad (4)$$

The reactivity trends in G3 and G4 dendrimers were analyzed by correlating the $k_{1,obs}$ values with the concentration of free amino groups calculated from the potentiometric titration data. Fig. 9(a) and (b) show the plots of $k_{1,obs}$ *vs.* concentration of free amino groups, which are linear and slopes corresponding to the $k^n_{2,Nu}$ values given in Table 2. These plots cover the pH range from 6 to 10 where, by analogy with G0 and G1, the pK_a values should vary from *ca.* 8 to *ca.* 10 and the observed linearity indicates that all amino groups, independently of their basicity, react with NPA with a single $k^n_{2,Nu}$ value as observed for G0.

As a result from this analysis, we find a 3.5-fold rate enhancement at pH 8.5 for G3 compared to the reference compound (Fig. 6(a)), instead of a 28-fold previously reported effect.[7] It seems that the cause of the discrepancy is a much smaller rate constant for NPA aminolysis by the reference compound, AcEn, estimated in ref. 7*b* From this study, performed by initial rates at a single pH value, one may estimate from the reported initial rate 4.03 × 10^{-10} M s^{-1} for 6.4 × 10^{-3} M En (which has the same reactivity as AcEn at pH 8.5) and using 1.4 × 10^{-5} M of NPA as substrate the second-order rate constant k'_2 = 0.00446 M^{-1} s^{-1} at pH 8.5. In contrast, we find k'_2 = 0.196 M^{-1} s^{-1} at the same pH (Fig. 4(a) and

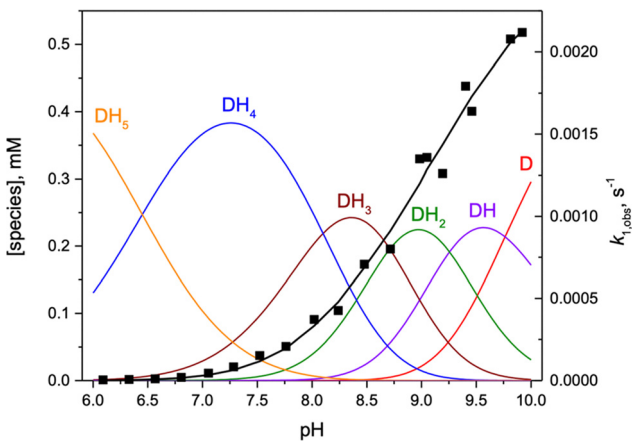

Fig. 7 Concentrations of differently protonated G0 dendrimer species *vs.* pH (solid lines, left *Y*-axis) superimposed with observed first-order rate constants of NPA aminolysis in the presence of 0.5 mM G0 at variable pH (solid squares, right *Y*-axis). The black solid line is the theoretical profile calculated with eqn (3) and parameters given in Table 2.

Table 2 Second-order rate constants per free amino group for dendrimers at different degrees of protonation in NPA aminolysis

	AcEn	G0				G1			G3	G4
$k^n_{2,Nu}$, M^{-1} s^{-1}	0.88	1.23	1.16	1.13	1.13	0.65	0.78	1.95	0.74	1.0
n		0	1	2	3	0–2	3–6	7	na	na
pK_a [a]	9.37	9.16	8.78	8.35	8.09	9.02–8.38	8.59–7.94	7.95	na	na

[a] Statistically corrected pK_a values per one amino group, na = not available.

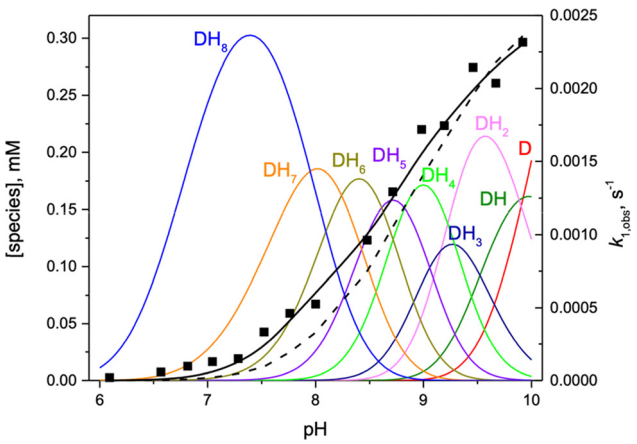

Fig. 8 Concentrations of differently protonated G1 dendrimer species *vs.* pH (solid lines, left *Y*-axis) superimposed with observed first-order rate constants of NPA aminolysis in the presence of 0.5 mM G1 at variable pH (solid squares, right *Y*-axis). The black solid line is the theoretical profile calculated with eqn (4) and parameters given in Table 2. The dashed line is the calculated profile assuming all species possess similar $k^n_{2,Nu}$ values.

Fig. S14) and our 44-fold larger value agrees with entire pH-profile of the rate constant. Also, the reported $k_{2,Nu}$ = 8.93 M^{-1} s^{-1} for En[19] corresponds to $k'_2 = 0.19$ M^{-1} s^{-1} at pH = 8.5 considering the known pK_a 10.18 of En. Second-order rate constants estimated from initial rates of NPA aminolysis by dendrimers reported in ref. 7*b* are smaller than the respective k'_2 values determined in the present work, but only by a factor of 3 attributable to a difference in experimental conditions.

4. DNFB aminolysis by dendrimers

Results for kinetics of DNFB aminolysis demonstrated less regular but generally similar pattern. Fig. 10 shows pH-profiles of k'_2 for all dendrimers and AcEn. The general pattern is similar to that for NPA (see Fig. 6(a)) but with a smaller *ca.* 8-fold dendritic effect at pH 7 observed only for higher-generation dendrimers G3 and G4. Lower-generation dendrimers G0 and G1 are less reactive than AcEn in completely neutral forms at high pH and approach the reactivity of the reference compound only at pH values below 8.

The rate *vs.* pH profiles superimposed with the species distribution diagrams for G0 and G1 are shown in Fig. 11(a) and (b), and the rate constants calculated from these data by using eqn (3) and (4) are summarized in Table 3.

The profiles of $k_{1,obs}$ *vs.* concentration of free amino groups for G3 and G4, as in the case of NPA are linear, Fig. 12(a) and (b), with slopes corresponding to $k_{2,Nu}$ values given in Table 3.

An inspection of Table 3 reveals that the reactivity of dendrimer amino groups towards DNFB is essentially independent of pK_a of their conjugated acid as in the case of NPA. For G0, $k^n_{2,Nu}$ value remains approximately constant for n = 0–2, and increases noticeably for n = 3 (*i.e.*, the tri-protonated species).

We observe therefore that, for reactions of nucleophilic substitution with two different substrates demonstrating "normal" Brønsted correlations of rate constants with pK_a values of conjugated acids of nucleophilic species, the reactivity of dendrimer amino groups is independent of pK_a of their conjugated acid. The reason of this effect, which is opposite to what is observed in aminolysis by polyamines of irregular structures like polypropylene amine,[8,9] is that the variation in pK_a for dendrimers occurs only due to long-range electrostatic interactions

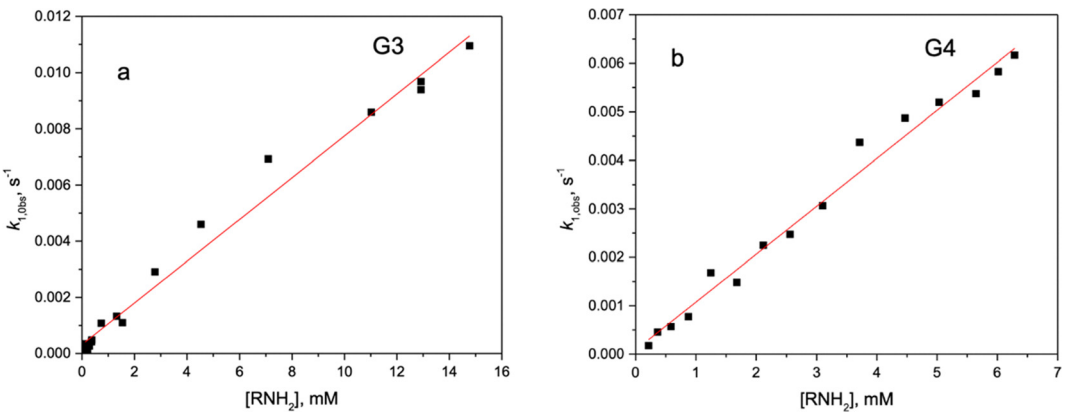

Fig. 9 Observed first-order rate constants for NPA aminolysis by dendrimers (a) G3 and (b) G4 at variable pH *vs.* concentration of neutral amino groups.

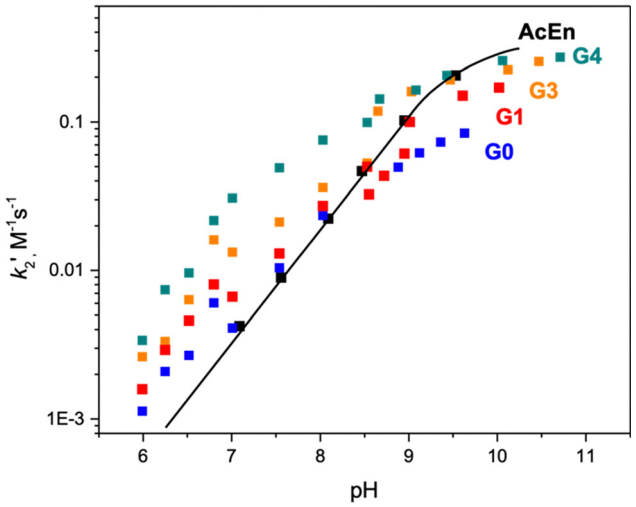

Fig. 10 Observed second-order rate constants, k_2', M^{-1} s^{-1}, of DNFB aminolysis by dendrimers and AcEn *vs.* pH.

without any contribution of short-range inductive or hydrogen bonding effects capable to affect the nucleophilic reactivity of neutral amino groups.

Comparing the results in Tables 2 and 3 one can notice that in the case of NPA as a substrate, the $k^n_{2,Nu}$ values for all dendrimers are very close to each other and to the $k_{2,Nu}$ of AcEn. In contrast, when DNFB is the substrate, dendrimers of lower generations are significantly less reactive than those of higher generations. A possible explanation for this difference is that larger dendrimers have a less "aqueous" interior, and the rate of the S_NAr reaction is more sensitive to medium effects than that of ester aminolysis.

5. Solvent effect in DNFB aminolysis and quantification of dendrimers.

Another possible factor affecting the reactivity of amino groups of dendrimers, besides shift in pK_a, is the medium effect created by the change in local solvation of reactants inside the dendrimer. Available data show a small difference in rates of ester aminolysis in water and MeCN mixtures, but there is a significantly larger rate in MeCN than in water for the reaction of amines with DNFB.[16] There are several studies of solvent effects on S_NAr reactions.[16] The rate of DNFB aminolysis in aprotic solvents increases as solvent polarity increases following a linear correlation with a positive slope when correlated with the Dimroth–Reichardt solvatochromic parameter $E_T(30)$.[15] With protic solvents a similar behavior was found for the reaction of DNFB with substituted anilines in MeOH – ethyl acetate mixtures. A linear correlation is observed for rate constants with E_T^N affording a positive slope and a large *ca.* 100-fold overall increase in rate constants in pure MeOH (E_T^N = 0.762) compared with pure ethyl acetate (E_T^N = 0.228).[21] The observed rate constants of the reaction of DNFB with morpholine in MeCN–water mixtures at low amine concentration, depend very little on the solvent composition but are significantly larger in MeCN at high amine concentrations because of the general-base assistance existing in MeCN but absent in water.[16,22] In order to evaluate the medium effect in our case, the rate constants of reactions of DNFB with AcEn and dendrimers were measured in DMSO–water mixtures at low 1 mM total concentration of amino groups, when general base assistance is insignificant. For these mixtures, three sets of empirical solvent parameters are available: the Dimroth–Reichardt solvatochromic parameter E_T^N[23] which reflects a cumulative effect of several types of solvent–solute interactions, the Kamlet–Taft parameters[24] based on solvent dipolarity/polarizability π*, acidity α, and basicity β[25] (eqn (5)) and the Catalán parameters involving solvent acidity SA, basicity SB, and polarity/polarizability SPP[26] (eqn (6)).

$$\log k = \log k_0 + s\pi^* + a\alpha + b\beta \quad (5)$$

$$\log k = \log k_0 + s\mathrm{SPP} + a\mathrm{SA} + b\mathrm{SB} \quad (6)$$

The reaction of AcEn and dendrimers G0, G1, G3 and G4 with DNFB was measured at DMSO molar fractions ranging from 0 to 1 and a total primary amine concentration of 1.0 mM (Fig. S15). Fig. 13(a) shows the profiles of log k_2' *vs.* molar fraction of DMSO in DMSO–water mixtures demonstrating

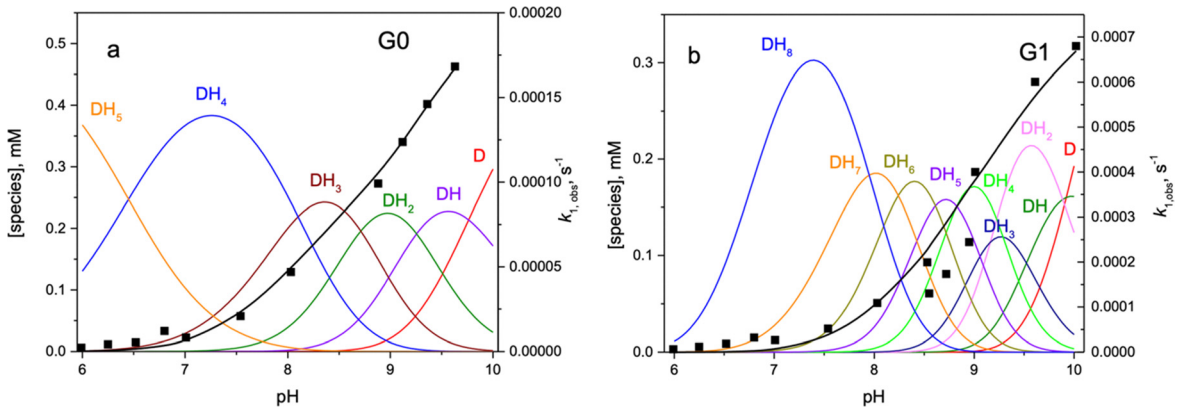

Fig. 11 Concentrations of differently protonated (a) G0 and (b) G1 dendrimer species *vs.* pH (solid lines, left *Y*-axis) superimposed with observed first-order rate constants for DNFB aminolysis in the presence of 0.5 mM dendrimers at variable pH (solid squares, right *Y*-axis). The black solid lines are the theoretical profile calculated with eqn (3) for G0 or (4) for G1 and parameters given in Table 3.

Table 3 Second-order rate constants per free amino group for dendrimers at different degrees of protonation in DNFB aminolysis

	AcEn	G0			G1		G2	G3
$k^n_{2,Nu}$, M^{-1} s^{-1}	0.31	0.10	0.12	0.08	0.20	0.19	0.25	0.42
n		0	1	2	3	0–7	na	na
pK_a [a]	9.37	9.16	8.78	8.35	8.09	9.02–7.95	na	na

[a] Statistically corrected pK_a values per one amino group, na = not available.

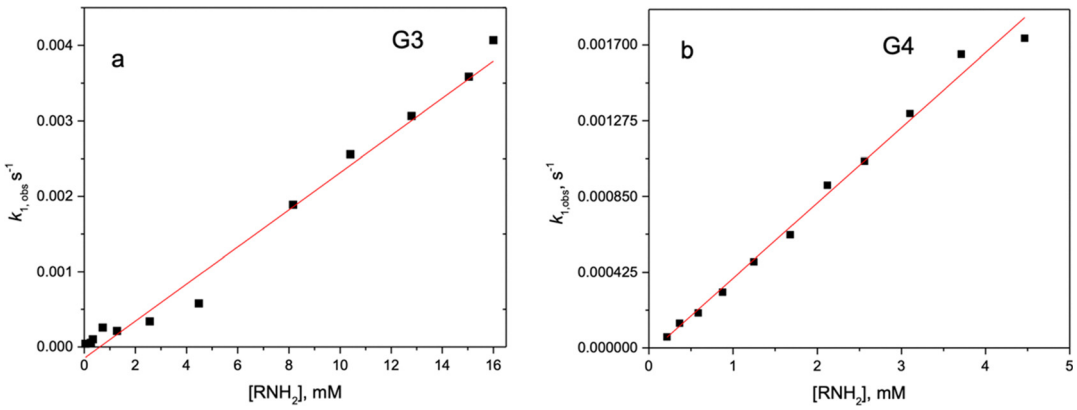

Fig. 12 Observed first-order rate constants for DNFB aminolysis by dendrimers (a) G3 and (b) G4 at variable pH *vs.* concentration of neutral amino groups.

large *ca.* 100-fold increase in the reaction rate in DMSO compared with water. There is an approximate linear correlation with E_T^N for all dendrimers and AcEn with a negative slope and regression coefficients Adj. R^2 varying from 0.91 to 0.99, Fig. 13(b). Interestingly this result is essentially opposite to the mentioned above solvent effect in methanol–ethyl acetate mixtures where the reaction rate is much faster in mixtures with a protic cosolvent than with an aprotic. The slopes of correlations in Fig. 13(b) are -4.6 ± 0.3 for AcEn and -4.3 ± 0.2; -4.7 ± 0.1; -3.4 ± 0.3; -3.3 ± 0.3 for G0, G1, G3 and G4 demonstrating smaller sensitivity of reactivity of dendrimers of higher generations to solvent composition. Thus, it seems that the reduced reactivity of lower-generation dendrimers, as compared with AcEn, results from some structural differences, *e.g.* a steric effect, which is compensated by positive medium effect in higher generation dendrimers. A steric effect may be more significant for DNFB than for NPA because in the transition state of the former (see Scheme 1) the amino group is positioned close to a voluminous aromatic ring of the substrate.

A more detailed analysis in terms of eqn (5) and (6) was performed for AcEn. Table 4 collects the obtained coefficients together with statistical parameters found by the multiple linear regression. The quality of the correlation, as judged by the values of Adj.R^2, is good for both equations, but the Kamlet–Taft correlation allows a more rational interpretation. Surprisingly, in both cases coefficients for solvent acidity and basicity, a and b, which describe opposite effects have the same negative sign. However, considering the usually accepted

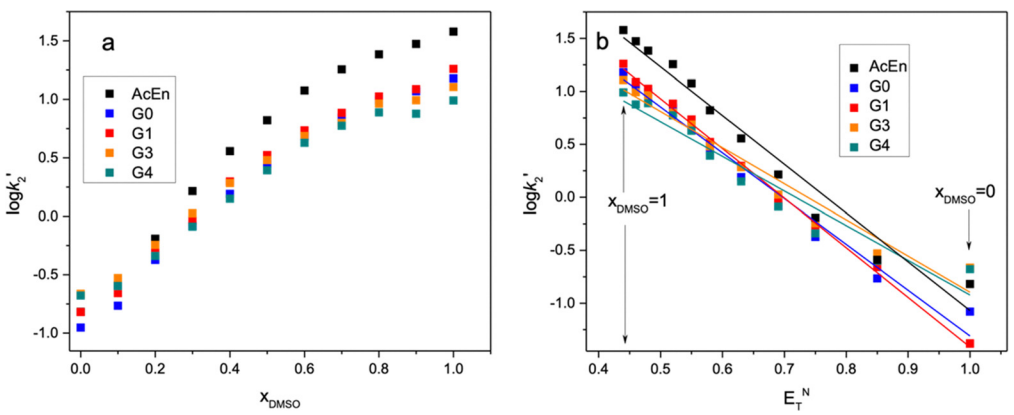

Fig. 13 (a) Logarithmic dependence of the observed second-order rate constant for the reaction of dendrimers and AcEn with DNFB in DMSO–water mixtures, (b) the correlation of log k_2', with Dimroth–Reichardt solvatochromic parameter E_T^N.

Table 4 Coefficients in eqn (5) and (6) obtained by multiple linear regressions of results in Fig. 13 for AcEn

Eqn (4)	$\log k_0$	s	a	b	Adj.R^2
Value	9.22	−7.5	−1.44	−0.24	0.987
Prob > $\|t\|$	0.0036	0.000333	0.023	0.90	

Eqn (5)	$\log k_0$	s	a	b	Adj.R^2
Value	13.8	−9.4	−5.1	−3.9	0.985
Prob > $\|t\|$	0.0032	0.0069	0.00021	0.0086	

threshold value of Prob > $|t|$ below 0.05, one can conclude that the coefficient b in the Kamlet–Taft correlation is statistically insignificant, and the physically meaningful effect is a negative a coefficient, that is the inhibitory effect of a solvent with higher acidity, in this case water. This can be interpreted as a stronger solvation of the nitrogen nucleophile by hydrogen bonding to water therefore reducing its reactivity. A very large negative coefficient s means a higher reactivity in a medium of lower polarity although its statistically significance may be exaggerated because both polarity indexes, π^* and SPP, show a very little variation, just by ±5% from a mean value of about 1 in the DMSO–water mixture.

The unexpectedly strong solvent effect prompted us to test the applicability of the reaction with DNFB as an analytical method for quantifying dendrimers. The traditional Sanger method requires a long reaction time, about 30 min even with heating (about 60 °C), and the removal of the absorbing hydrolysis by-product 2,4-dinitrophenol.[18,27] In comparison, a hundred times faster reaction is observed in DMSO: it is completed in just 5 min at room temperature in the presence of 1 mM DNFB and 1 mM of a ternary amine base, triethylamine or pyridine, added to neutralize the released HF (Fig. S16). Fig. 14 shows the calibration plots in the presence of dendrimers from which a detection limit LOD = 6 μM based on total amino groups can be estimated.

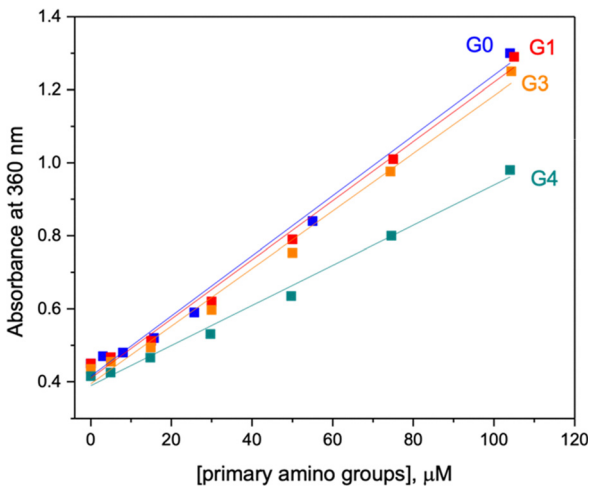

Fig. 14 Calibration plots for spectrophotometric determination of dendrimers in DMSO after 5 minutes of reaction at room temperature with 1 mM DNFB and 1 mM pyridine.

Conclusions

The nucleophilic reactivity of terminal amino groups in dendrimers of different generations, in their fully deprotonated forms at high pH, towards NPA is similar to that of the simple reference amine AcEn. However, at lower pH values with partially protonated species, the relative reactivity of dendrimers becomes higher than that of AcEn demonstrating a 15-fold dendritic effect at pH about 7. A similar behavior is observed with DNFB as substrate, although with a smaller relative reactivity for low-generation dendrimers in their fully deprotonated forms and a lower dendritic effect, *ca.* 10-fold, at pH about 7. The stepwise increase in the protonation state of the dendrimers induces a decrease in the subsequent pK_a values of their protonated amino groups, but the individual rate constants calculated for neutral amino groups within differently protonated species remain unaffected. Therefore, the dendritic effect can be attributed entirely to the increased fraction of neutral amino groups in the protonated dendrimer species, due to the decrease in the pK_a of protonated amino groups. In this aspect, dendrimers behave differently from polyamines like poly(ethyleneimine) or polyallylamine, in which a decrease in pK_a also induces a decrease in the reactivity of amino groups in accordance with the Brønsted correlation. This difference can be attributed to weaker interactions between protonated and neutral amino groups in dendrimers, because of larger distances between amino groups in dendrimers. So, the decrease in pK_a in this case is a result of only long-range electrostatic effect which does not reduce the intrinsic nucleophilic reactivity. The study of the solvent effect on the reaction of dendrimers with 2,4-dinitrofluorobenzene, conducted for the interpretation of our kinetic results, led to the development of a new, sensitive method for the quantification of PAMAM-NH_2 dendrimers in a μM concentration range in DMSO solution.

Experimental section

General remarks

The amine terminated PAMAM dendrimers ethylenediamine core generations G0, G1, G3 and G4, were purchased from Sigma Aldrich as solution in methanol and were used with no further purification; the concentration of all dendrimers was tested by titration with standardized HCl and back titration with standardized NaOH under N_2 atmosphere at 25 °C. The amines ethylenediamine (En), *N*-acetyl ethylenediamine (AcEn), *N*-methyl ethylenediamine (MeEn) and the substrates were purchased from Sigma Aldrich and purified by recrystallation. The stock solutions of dendrimers and amines were prepared by weighting the dried ammount and, as well as the amines, dissolved it in Barnstead nano pure distilled and deionized water. Stock solutions of substrates NPA and DNFB were prepared in acetonitrile. A digital pH meter Orion 710A connected to an Orion ROSS Ultra 8103BN pH combination glass electrode was used for pH measurements and the reversibility of all titrations were confirmed. Reaction kinetics were

performed at 25 °C and were monitored by UV-vis spectroscopy using a Hewlett–Packard 8453 diode-array spectrophotometer with a thermostated multicell sample compartment (± 0.1 °C) using quartz cuvettes.

Potentiometric titrations

Potentiometric titrations of dendrimers were performed on a 5 mL thermostated cell using a total R-NH_2 terminal amine concentration of 10 mM under N_2. To calculate the cumulative stability constants, the data were fitted using Hyperquad software Ver.5.2.19.[28] The obtained pK_a values were compared with the theoretical ones calculated with ACD Labs Percepta 2023.1.2 using both, Classic and Galas methods, and with the previously reported values.[10–13]

Kinetic measurements

The pH in the kinetic measurements was kept constant by 50 mM solutions of biological non-coordinating buffers (MES, MOPS, EPPS, CHES, and CAPS) used in appropriate pH intervals with NPA as substrate and phosphate and borate buffers were used with DNFB as substrate to avoid the presence of reactive secondary amine groups of CHES and CAPS; a constant pH was confirmed by initial and final pH readings of each kinetic run. In all experiments a large excess of the nucleophile over the substrate was employed, ensuring the observed first-order reaction kinetics. Kinetic curves, examples shown in Fig. S8–S11, were fitted to a first order rate reaction integrated equation to obtain observed first order rate constants $k_{1,obs}$ or by the initial rate method for slow reactions. Each kinetic run was performed 3 times and 2–3 series of data at variable pH or concentration values within the same range were measured as illustrated in Fig. S12 for NPA aminolyis with dendrimer G4. The proportionality of $k_{1,obs}$ to the total nucleophile (primary amine groups) concentration was confirmed for all dendrimers and AcEn. Therefore, the observed second-order rate constants k_2' were calculated dividing $k_{1,obs}$ by the total amine concentration. For NPA and DNFB, a concentration of 0.05 mM of substrate was used and the course of the reactions were monitored by measuring the release of 4-nitrophenol at 400 nm or formation of 2,4-dinitrophenylated amine at 360 nm. At variable pH, the background rate constants in the absence of amine were negligible, even though they were subtracted from the observed rate constants to give only the aminolysis parameters. The rate constant of alkaline hydrolysis of DNFB k_{OH} = 0.18 M^{-1} s^{-1} affording 2,4-dinitrophenolate anion (DNP) was measured independently in 10 mM NaOH and the alkaline hydrolysis contribution was subtracted from the observed rate constant. Since the UV-vis spectra of DNP and the 2,4-dinitrophenylated amine products are almost identical in the monitored region, the formation of the addition product was confirmed by acidifying with HCl at the end of each run (Fig. S13).

Author contributions

A. López-Pacheco: data curation, formal analysis, investigation, writing – original draft, review & editing. E. Alpizar-Juárez: data curation, formal analysis, investigation. P. Gómez-Tagle: conceptualization, data curation, formal analysis, funding acquisition, validation, writing – original draft, review & editing, visualization. A. K. Yatsimirsky: conceptualization, data curation, formal analysis, funding acquisition, validation, visualization, writing – original draft, review & editing.

Conflicts of interest

There are no conflicts to declare.

Data availability

The datasets supporting this article, including kinetic, spectrophotometric, and potentiometric titration results are provided in the supplementary information (SI). See DOI: **https://doi.org/10.1039/d5nj02642c**.

Acknowledgements

The financial support from the Universidad Nacional Autónoma de México through the Programa de Apoyo a Proyectos de Investigación e Innovación Tecnológica grant (PAPIIT-UNAM Project IN221321) and the Programa de Apoyo a la Investigación y el Posgrado de Facultad de Química (PAIP 5000-9161 and PAIP 5000-9042) is gratefully acknowledged. A. P. López-Pacheco and E. Alpizar-Juárez thanks the Consejo Nacional de Humanidades, Ciencias y Tecnologías (CONAHCyT, México) for the Graduate Fellowships.

References

1 D. Astruc and F. Chardac, *Chem. Rev.*, 2001, **101**, 2991–3023.
2 C. Liang and J. M. J. Fréchet, *Prog. Polym. Sci.*, 2005, **30**, 385–402.
3 (*a*) P. J. Gittins and L. J. Twyman, *Supramol. Chem.*, 2003, **15**, 5–23; (*b*) M. Raynal, P. Ballester, A. Vidal-Ferran and P. W. N. M. van Leeuwen, *Chem. Soc. Rev.*, 2014, **43**, 1734–1787.
4 A.-M. Caminade, A. Ouali, M. Keller and J.-P. Majoral, *Chem. Soc. Rev.*, 2012, **41**, 4113–4125.
5 L. J. Twyman, A. S. H. King and I.-K. Martin, *Chem. Soc. Rev.*, 2002, **31**, 69–82.
6 D. J. Evans, A. Kanagasooriam, A. Williams and R. J. Pryce, *J. Mol. Catal.*, 1993, **65**, 21–32.
7 (*a*) I. K. Martin and L. J. Twyman, *Tetrahedron Lett.*, 2001, **42**, 1123–1126; (*b*) J. L. Burnett, A. S. H. King, I. K. Martin and L. J. Twyman, *Tetrahedron Lett.*, 2002, **43**, 2431–2433; (*c*) J. Burnett, A. S. H. King and L. J. Twyman, *React. Funct. Polym.*, 2006, **66**, 187–194.
8 A. Arcelli and C. Concilio, *J. Org. Chem.*, 1996, **61**, 1682–1688.
9 E. A. Castro, G. R. Echevarria, A. Opazo, P. S. Robert and J. G. Santos, *J. Phys. Org. Chem.*, 2006, **19**, 129–135.

10 D. Cakara, J. Kleimann and M. Borkovec, *Macromolecules*, 2003, **36**, 4201–4207.
11 A. Buczkowski, P. Urbaniak, J. Stawowska, S. Romanowski and B. Palecz, *J. Mol. Liq.*, 2012, **171**, 54–59.
12 U. Böhme, A. Klenge, B. Hänel and U. Scheler, *Polymers*, 2011, **3**, 812–819.
13 K. A. Krot, A. F. Danil de Namor, A. Aguilar-Cornejo and K. B. Nolan, *Inorg. Chim. Acta*, 2005, **358**, 3497–3505.
14 Y. Liu, V. S. Bryantsev, M. S. Diall and W. A. Goddard III, *J. Am. Chem. Soc.*, 2009, **131**, 2798–2799.
15 N. S. Nudelman, P. M. E. Mancini, R. D. Martinez and L. R. Vottero, *J. Chem. Soc., Perkin Trans. 2*, 1987, 951–954.
16 I. H. Um, S. W. Min and J. M. Dust, *J. Org. Chem.*, 2007, **72**, 8797–8803.
17 I. H. Um, L. R. Im, J. S. Kang, S. S. Bursey and J. M. Dust, *J. Org. Chem.*, 2012, **77**, 9738–9746.
18 E. Athanasiou-Malaki, M. A. Koupparis and T. P. Hadjiioannou, *Anal. Chem.*, 1989, **61**, 1358–1363.
19 W. P. Jencks and M. Gilchrist, *J. Am. Chem. Soc.*, 1968, **90**, 2622–2637.
20 R. Ormazábal-Toledo, R. Contreras, R. A. Tapiab and P. R. Campodónicoc, *Org. Biomol. Chem.*, 2013, **11**, 2302–2309.
21 J. Jamali-Paghaleh, A. R. Harifi-Mood and M. R. Gholami, *J. Phys. Org. Chem.*, 2011, **24**, 1095–1100.
22 A. Valvi and S. Tiwari, *J. Phys. Org. Chem.*, 2017, **30**, e3615.
23 T. M. Krygowski, P. K. Wrona, U. Zielkowska and C. Reichardt, *Tetrahedron*, 1985, **41**, 4519–4527.
24 Y. Marcus, *J. Chem. Soc., Perkin Trans. 2*, 1994, 1751–1758.
25 M. J. Kamlet, J.-L. M. Abboud, M. H. Abraham and R. W. Taft, *J. Org. Chem.*, 1983, **48**, 2877–2887.
26 J. Catalán, C. Díaz and F. García-Blanco, *J. Org. Chem.*, 2001, **66**, 5846–5852.
27 H. Hegedus, A. Gergely, T. Veress and P. Horváth, *Analysis*, 1999, **27**, 458–463.
28 P. Gans, A. Sabatini and A. Vacca, *Talanta*, 1996, **43**(10), 1739–1753.